Summer 5-1-2024

The Future Of Brain Tumor Diagnosis: CNN And Transfer Learning Innovations

Shengyuan Wang
wsy20030518@126.com

The Future of Brain Tumor Diagnosis: CNN and Transfer Learning Innovations

Shengyuan Wang

Susan Fox, Advisor

Lian Duan, Reader

Will Mitchell, Reader

MACALESTER

Department of Mathematics, Statistics, and Computer Science

May, 2024

Abstract

For the purpose of improving patient survival rates and facilitating efficient treatment planning, brain tumors need to be identified early and accurately classified. This research investigates the application of transfer learning and Convolutional Neural Networks (CNN) to create an automated, high-precision brain tumor segmentation and classification framework. Utilizing large-scale datasets, which comprise MRI images from open-accessible archives, the model exhibits the effectiveness of the method in various kinds of tumors and imaging scenarios. Our approach utilizes transfer learning techniques along with CNN architectures strengths to tackle the intrinsic difficulties of brain tumor diagnosis, namely significant tumor appearance variability and difficult segmentation tasks. The segmentation model, based on the U-Net architecture, excels in delineating tumor boundaries with remarkable precision, while the classification model, employing EfficientNet B3, achieves high accuracy in identifying tumor types. Our findings indicate a significant improvement in the speed and accuracy of brain tumor diagnosis, offering potential benefits for clinical practice and patient care.

Acknowledgments

I want to express my deepest gratitude to my advisor, Susan Fox, for her invaluable support throughout my research. Her generosity in providing access to the robot lab has been instrumental in the progress and success of my work. I am profoundly thankful for our insightful conversations about computer vision, which have greatly enhanced my understanding and enriched my research experience.

I would also like to thank all of my committee members for providing helpful feedback on my capstone and honors thesis. Their meticulous reviews and comments considerably improved the quality of my work and improved its outcome. Their advice and encouragement have been invaluable to my academic career, and I am very grateful for their patience and support.

My thanks extend to all my professors at Macalester College for their excellent teaching over the past three years. The knowledge and insights I have gained from their instruction have been fundamental to both my academic and personal growth. Their commitment to creating a supportive and intellectually stimulating environment has profoundly enriched my educational experience. I must also convey my gratitude to my friends and family. Their encouragement and support have helped me stay on track academically. Thank you for your support and contribution to my success.

Contents

Chapter 1

Introduction

In the changing field of medical science and technology, information technology and e-healthcare systems have revolutionized the way clinical professionals diagnose and treat diseases [25]. Among the challenges encountered in the medical industry, the segmentation and classification of brain tumors from magnetic resonance imaging (MRI) images stand out because of their complexity and the importance of fast and precise diagnosis.

MRI is a medical imaging method used in radiology to study the structure and function of the human body [11]. It can offer detailed images of the body in three dimensions. It is particularly beneficial in neurological, musculoskeletal, and cancer imaging because it provides better contrast between the body's soft tissues than computer tomography (CT). Several contemporary challenges in image-guided surgery, therapy evaluation, and diagnostic tools benefit from accurate 3D representations of anatomical structures [11].

Most research in developed countries has shown that the death rate of people affected by brain tumors has increased over the last 30 years. Brain tumors are currently one of the leading causes of death in children and adults. Brain tumors, which are defined by the uncontrolled growth of cells in the brain, can be malignant (cancerous) or benign (non-cancerous), as shown in Table 1.1, and their detection and classification are critical in establishing the best course of therapy. The World Health Organization and the American Brain Tumor Association classify brain tumors into four classes: low-grade (benign) tumors (grades I and II) and high-grade (malignant) tumors (grades III and IV) [6]. Grade I brain tumor cells resemble normal cells, which grow slowly and are less prone to spreading. Grade II tumor cells are prone to spreading into surrounding brain tissue. Grade III

and IV cells are abnormal, can migrate to other sections of the brain, and are often the fastest-growing tumors that recur after therapy, indicating that they are cancerous or malignant. The difference between these grades is important because it influences treatment decisions and patient outcomes.

Characteristic	Benign	Malignant
Nature	Not cancerous	Cancerous
Tissue Invasion	Not invade	Invade
Spread	Not spread	Spread
Growth Rate	Slow	Fast
Recurrence	Not likely to recur	More likely to recur
Shape	Smooth, regular shape	Irregular shape
Mobility	Move around	Not move around

Table 1.1 Comparison of Benign and Malignant Tumors

Identification in the context of brain tumors with magnetic resonance images (MRI) includes recognizing the presence of tumors discerning their characteristics and grading their severity. This level of detail is critical for medical diagnosis because it provides the anatomical structures and any potential tissues. Such comprehensive information is important for formulating treatment plans and monitoring the patient's progress.

Segmentation is the process of dividing an image into sections based on pixels with comparable features. Manual segmentation of diseased brain tissues from normal tissues takes a long time and can yield false results [11]. The precise segmentation of brain tumors serves a critical function beyond diagnosis. It is vital for creating detailed models of pathological brains [1] and enhancing the accuracy of brain atlases [2] [22]. Despite major advances in medical imaging technology, segmenting and classifying brain tumors remains difficult. The variability of tumor concerns, combined with their potential to arise anywhere in the brain and resemble normal tissues, complicates the diagnostic process. Traditional methods in medical imaging largely rely on the manual segmentation performed by radiologists, a process that is highly susceptible to human error and subjective interpretation.

[1] The study of diseases and disorders related to the brain

[2] Serial sections along different anatomical planes of the healthy or diseased developing or adult animal or human brain

This manual technique involves the radiologist outlining areas of interest in medical images, such as MRI scans or CT images, by hand. Due to the complex nature of these images and the variability in human perception, this segmentation is often inconsistent with different potentially producing varying results from the same image. These inconsistencies can lead to mistakes in how images are interpreted, which in turn may affect the accuracy of the diagnoses derived from them. Furthermore, such errors can propagate through the medical workflow, impacting treatment decisions and ultimately patient outcomes.

This paper addresses these issues and provides insights into the limitations of present approaches, as well as the potential for convolutional neural networks (CNN) and transfer learning to automate the segmentation process and improve the accuracy of existing methods. The importance of early and accurate identification of brain cancers cannot be overemphasized. The risks for patients are extremely high, as the tumor has the potential to develop from low to high grade if not treated promptly. This study highlights the limitations of current manual and semi-automated segmentation approaches, emphasizing the need for a more dependable and more efficient alternative.

The primary aim of this research is to demonstrate the effectiveness of a CNN and transfer learning-based approach for the segmentation and classification of brain tumors. This exploratory and interpretative study sets forth four specific objectives:

- To automate the segmentation and classification process
- To improve upon existing methods in terms of accuracy and efficiency
- To prove the method's effectiveness across large datasets and complex structures
- To enhance the diagnostic process for brain tumors.

In this study, we developed and validated an automated framework for the segmentation and classification of brain tumors using MRI images with CNN and enhanced with Transfer Learning (TL) techniques. Utilizing comprehensive datasets from publicly accessible Kaggle repositories, our approach employs the 3D U-Net architecture for precise tumor boundary segmentation and EfficientNet B3 for robust tumor type classification, categorizing tumors into glioma, meningioma, no tumor, and pituitary classes.

The performance of our models demonstrates the effectiveness of the segmentation model achieving an accuracy of over 99%, and the classification model surpassing expectations with an accuracy of over 99%.

The paper is organized as follows: the subsequent sections focus on a detailed analysis of the proposed approach, simulation results, and performance evaluation; the comparative analysis highlights the advantages and limitations of the study; and the paper concludes with insights on the future scope of this research.

Chapter 2

Background and Related Works

2.1 Medical Backgrounds

2.1.1 Magnetic Resonance Imaging Overview

Magnetic Resonance Imaging (MRI) represents an important advancement in medical diagnostics using strong magnetic fields and radio waves to visualize the complex structure within the human body [21]. The non-invasive imaging technique uses a series of electromagnetic fields [21]:

- A strong static field to polarize hydrogen nuclei
- A spatially variable field for encoding spatial information
- A weak radio frequency field to manipulate hydrogen nuclei

These electromagnetic fields can produce signals that are captured to generate detailed images of bodily tissue. This sophisticated approach allows for the differentiation of tissue characteristics, which is crucial for various medical diagnoses and research applications.

MRI employs a variety of techniques [12] to illuminate the intricate structures within the body, each with its unique approach to imaging. Among these, T1-weighted, T2-weighted, DWI (Diffusion Weighted Imaging), and FLAIR (Fluid Attenuated Inversion Recovery) sequences are particularly notable. The contrast and detail in the images produced by these sequences are significantly influenced by two key parameters: the Time to Echo (TE) and the Repetition Time (TR) [12].

As shown in Table 2.1, T1-weighted images, which excel in showcasing anatomical details, use a short TE (typically less than 20 milliseconds) and a

Characteristic	T1-weighted	T2-weighted	DWI	FLAIR
Brightness of Fluid	Dark	Bright	Variable	Suppressed
Anatomical Detail	Excellent	Good	Fair	Good
Edema Sensitivity	Low	High	High	Very High
Lesion Detection	Good	Very Good	Excellent in acute phase	Excellent near CSF
Preferred Use	Anatomy visualization	Fluid detection	Ischemia detection	Lesion detection near CSF
Time to Echo (TE)	Short (<20 ms)	Long (>80 ms)	Variable	Long (90-150 ms)
Repetition Time (TR)	Short (400-600 ms)	Long (2000-6000 ms)	Variable	Very Long (>5000 ms)

Table 2.1 MRI Techniques: Key Parameters and Use Cases

shorter TR (ranging from 400 to 600 milliseconds). This combination helps make fat and other substances brighter to easier visualize the brain's structure, muscles, and fat. T2-weighted images, in contrast, utilize a longer TE (often greater than 80 milliseconds) and a longer TR (usually 2000 to 6000 milliseconds) to accentuate fluids and tissues to detect fluid accumulations, edema, and various pathologies. DWI focuses on the movement of water molecules within tissues and uses TE and TR values that can vary widely depending on the specific clinical application. The sensitivity of DWI to water diffusion makes it particularly useful for identifying acute ischemic strokes, the sudden blockages of blood vessels in the brain that lead to restricted blood flow, and tissue damage. This imaging technique is also adept at differentiating between cystic and solid lesions. FLAIR imaging, an advanced form of T2-weighted imaging, employs a long TE (90-150 milliseconds) and a very long TR (often greater than 5000 milliseconds) to suppress the signal from free fluids[1]. Each MRI sequence has the variable relaxation times of tissues under a magnetic field, guided by carefully chosen TE and TR values. In this way, clinicians have the detailed information they need for diagnosis and treatment planning.

2.1.2 Brain tumors Overview

Brain tumors, defined by the uncontrolled proliferation of cells within the brain, present a significant health challenge because of the critical functions of the location. The tumors can originate from various types of brain cells or be spread from cancers in other body parts, resulting in a mass that will compress or invade surrounding brain tissues.

[1]Free fluids refers to any bodily fluids that are not bound within cells or contained within a closed circulatory system, such as blood vessels or lymphatic channels. In medical imaging, this term is often associated with fluids that accumulate or are present in spaces where they are not typically abundant under normal physiological conditions

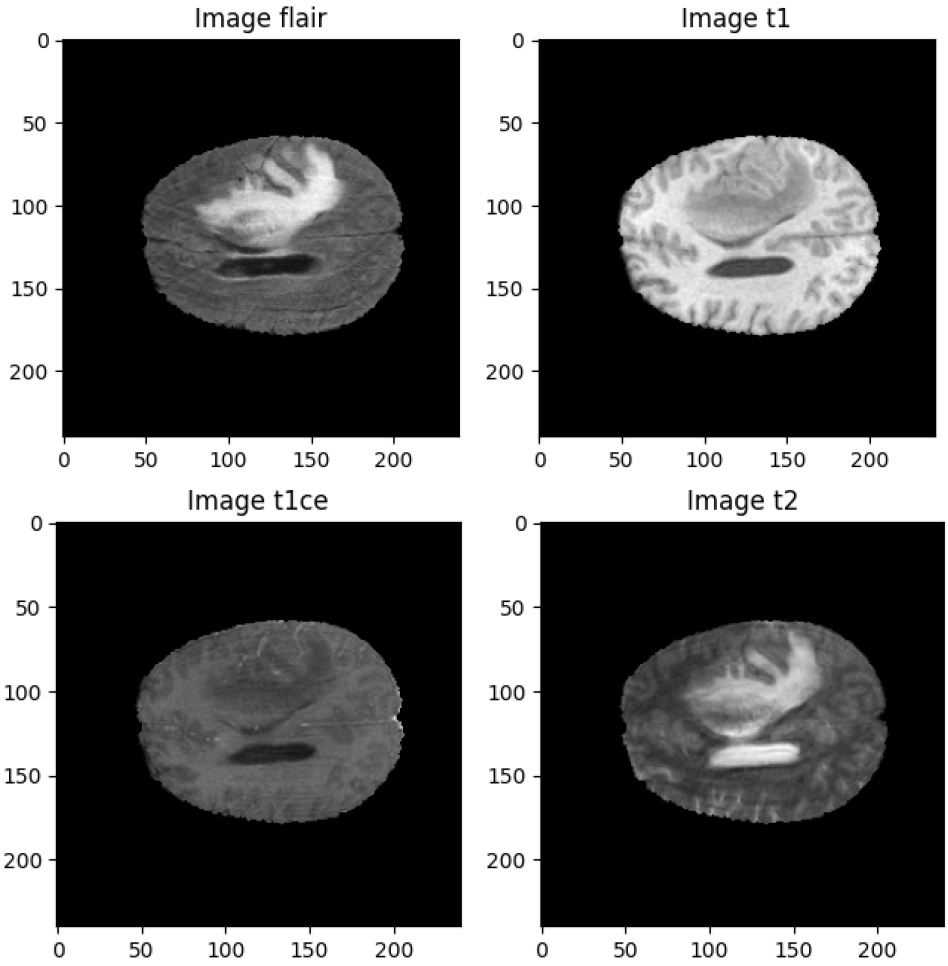

Figure 2.1 FLAIR, T1, T2, TICE Illustrations[20] For the same scan on the same brain

In MRI imaging of brain tumors, two significant components are often discussed: the tumor core and the enhancing part of the tumor:

- Tumor Core refers to the solid, central part of the tumor where the cell density is highest. The core is often hypoxic (low in oxygen) and necrotic (containing dead cells) due to rapid growth that outpaces blood supply. Its characteristics are crucial in determining the aggressiveness of the tumor and guiding the surgical approach, as removing the core can be important for treatment success.

- Enhancing part is the bright region surrounding the tumor core on T1-weighted MRIs following contrast agent injection. The enhancement is due to the leaky blood vessels typical of malignant growth, which allow the contrast agent to permeate. This part of the tumor is active, with cells proliferating at a high rate, and its extent helps in assessing the tumor's spread and the effectiveness of treatments like chemotherapy and radiation.

Brain tumors can be categorized based on the origin, location, and whether they are benign (non-cancerous) or malignant (cancerous), with common types including gliomas, medulloblastomas, meningiomas, craniopharyngiomas, and pituitary adenomas. The classification is important in determining the treatment strategy and prognosis:

- Gliomas originate from glial cells within the brain and include a range of subtypes, from low-grade to high-grade malignancies, requiring treatments that may involve surgery, radiation, and chemotherapy.
- Medulloblastomas are extremely malignant tumors in the cerebellum that primarily affect children and require serious treatment.
- Meningiomas are benign tumors that develop from the meninges which surround the brain. They do not require treatment, but if they are symptomatic, surgery or radiation may be necessary.
- Craniopharyngiomas are benign tumors near the pituitary gland that affect hormone levels. They are treated with surgery and radiation to reduce hormonal and neurological consequences.
- Pituitary adenomas are normally benign tumors of the pituitary gland. They can cause a variety of symptoms depending on their hormonal activity and should be seriously treated.

2.2 Convolutional Neural Network (CNN) Background

2.2.1 CNN Overview

Neural networks are a necessary part of artificial intelligence that has influenced how we solve complicated problems across a variety of fields. To imitate the human brain's complex network of neurons, neural networks are made up of layers of interconnected nodes. Each of the nodes is designed

to conduct a certain task. These networks transfer data by these nodes to allow them to learn and make decisions depending on the information they receive. A neural network includes three main layers: the input layer, hidden layers, and the output layer. The architecture enables the network to detect subtle patterns and correlations between datasets.

Convolutional Neural Networks (CNNs) are the neural networks that are very effective at analyzing visual input such as images. CNNs work by applying a set of filters to input images. These filters detect spatial hierarchies in data by learning from the input's small spatial areas while preserving spatial relationships between pixels[16]. This makes CNNs ideal for tasks involving massive images, where detecting local characteristics like edges and textures is critical for classification and analysis.

Each layer in a CNN converts one volume of activations to another using a differentiable function, allowing complex feature extraction from input data. Consider an input volume of size 32 * 32 * 3, which represents a 32 * 32 pixel image with three color channels. A convolutional layer might apply 10 filters of size 5 * 5 * 3 to this input. Each filter scans the input by sliding over it spatially, computing the dot product between the filter and input patches, resulting in a new 2D activation map for each. If no padding is utilized and the stride is one, each 5 * 5 * 3 filter converts the 32 * 32 * 3 input volume to a 28 * 28 activation map. Stacking the activation maps from all 10 filters results in an output volume of 28 * 28 * 10.

Convolutional layers in a CNN use many filters to capture various patterns within the input image, such as edges, textures, and contrasts—crucial features for medical imaging tasks like brain tumor segmentation. For example, early layers may detect simple edges or blobs, while deeper layers might identify more complex structures, such as the irregular shapes and boundaries typical of tumors.

Following the convolutional layers, pooling layers reduce the dimension of the data. This reduction not only decreases the computational load but also enhances the network's ability to detect features invariant to scale and orientation changes. In my study, max pooling layers could help the network maintain the detection of critical features like tumor boundaries, regardless of their scale or orientation in different MRI scans.

Finally, the fully connected layers synthesize the features extracted by the convolutional and pooling layers to make segmentation for the brain scan. In the context of brain tumor segmentation, these layers may detect whether an area of the image has a tumor and identify it as glioma or meningioma based on the patterns learned during training. This method involves

combining the localized and abstracted properties into a single prediction, allowing the network to accurately segregate and identify various tumor areas within the brain.

2.2.2 Functions and Optimizer in Neural Network Training

Rectified Linear Unit Activation Function

The Rectified Linear Unit (ReLU) activation function is fundamental in the setup of modern neural networks, especially those applied to deep learning. To address the vanishing gradient problem that plagued earlier activation functions such as sigmoid or tanh, ReLU provides a non-linear function that is zero for all negative inputs and linear for all positive inputs, given in Equation 2.1.

$$f(x) = \max(0, x) \tag{2.1}$$

Its simplicity enables faster training by successfully propagating gradients without significant loss as layers rise. Furthermore, ReLU contributes to the conservation of a sparse network, lowering the risk of over-fitting. The function's ability to accelerate the convergence of the stochastic gradient descent method is a key reason for its widespread adoption in network designs.

Adam Optimizer

The Adam optimizer is a method that computes individual adaptive learning rates for different parameters from estimates of the first and second moments of the gradients. Its name derives from "adaptive moment estimation," and it combines the advantages of two other extensions of stochastic gradient descent: AdaGrad, which works well with sparse gradients, and RMSProp, which handles non-stationary objectives effectively. Adam stores the decaying average of past squared gradients (v) and the decaying average of past gradients (m). Unlike standard stochastic gradient descent, which maintains a single learning rate for all weight updates, Adam adjusts the rate for each weight based on the computations of these averages, thus aiding in a more efficient optimization of the learning process. The method is well-regarded for its performance across a wide range of deep learning contexts and is known for requiring less memory and being computationally efficient.

Categorical Cross entropy Loss Function

Categorical cross-entropy, often utilized in multi-class classification problems, measures the difference between two probability distributions - predicted probability and actual distribution in the target variable. The function is especially suited for models predicting the probability of membership to multiple classes, where each target class label is one-hot encoded such as converting into a binary vector. It calculates the loss by taking the negative log of the probability assigned to the true class and summing this across all samples, effectively pushing the model to increase the probability assigned to the correct class labels while minimizing those assigned to incorrect labels. This loss function is fundamental in tasks where the outputs are probabilities that sum to one, as is typical in classification problems involving three or more class labels, such as in natural language processing or image categorization tasks.

2.3 Transfer Learning

In machine learning, traditional methods have used patterns from training data to predict future outcomes across various applications. These conventional approaches assume that the training and testing data share similar input feature space and distribution. However, differences in data distribution between training and test datasets can significantly affect the performance of predictive models. This disparity underscores the need for a methodology that can bridge the gap between differing domains, which sets the stage for the application of transfer learning.

Transfer learning addresses these challenges by enhancing the performance of a learner in a target domain through the transfer of knowledge from a related source domain. For instance, models trained on large, comprehensive datasets possess generalizable features that can be adapted to a new, but similar task with minimal adjustments. This is commonly seen in areas such as computer vision and natural language processing. In computer vision, a model trained to recognize objects in photographs can be fine-tuned to recognize specific items in satellite images. In NLP, models such as Bidirectional Encoder Representations from Transformers (BERT), originally trained on vast text corpora, are fine-tuned to perform specific linguistic tasks like sentiment analysis or language translation with more accuracy and less training time than training a model from scratch.

Transfer learning can significantly reduce the computational resources

and time required for training models, making sophisticated machine-learning applications more accessible and sustainable. Additionally, by starting with a model pre-trained on a large dataset, the performance on the new task is often better when the available training data is sparse. The approach can not only speed up the development process but also enhance the model's accuracy and reliability.

2.3.1 Evaluation Metrics Overview

- Accuracy, shown as Equation 2.2, measures the proportion of true results (both true positives and true negatives) among the total number of cases examined. It provides a simple indicator of the overall correctness of the model. For Equation 2.2, 2.3, 2.4, 2.6, TP denotes true positive, FP denotes false positive, FN denotes false negative, and TN denotes true negative.

$$\text{Accuracy} = \frac{\text{TP} + \text{TN}}{\text{Total Number of Cases}} \tag{2.2}$$

- Precision, shown as Equation 2.3, assesses the model's ability to identify only relevant instances among those instances it classified positively. High precision implies a low false positive rate.

$$\text{Precision} = \frac{\text{TP}}{\text{TP} + \text{FP}} \tag{2.3}$$

- Recall, shown as Equation 2.4, measures the model's ability to identify all relevant instances, providing insight into what proportion of actual positives was correctly identified.

$$\text{Recall} = \frac{\text{TP}}{\text{TP} + \text{FN}} \tag{2.4}$$

- F1-Score, shown as Equation 2.5, is the harmonic mean of precision and recall, offering a balance between the two by considering both the false positives and false negatives. It is particularly useful when the class distribution is uneven.

$$\text{F1-Score} = 2 \times \frac{\text{Precision} \times \text{Recall}}{\text{Precision + Recall}} \tag{2.5}$$

- The Dice Coefficient, shown as Equation 2.6, often used for spatial overlap metrics, is similar to the F1-Score but is typically used for comparing the pixel-wise agreement between a predicted segmentation and its corresponding ground truth.

$$\text{Dice} = \frac{2 \times \text{TP}}{2 \times \text{TP} + \text{FP} + \text{FN}} \tag{2.6}$$

- HD95 measures the maximum distance between the predicted and true boundaries of segmentation. It is robust against outliers by considering only the 95th percentile, thus providing a more stable measure of the spatial discrepancy in segmentation tasks.

- IoU, also known as the Jaccard index, measures the overlap between two boundaries. As indicated in Equation 2.7, it divides the area of overlap between the predicted segmentation and the ground truth by the area of their union, offering a clear measure of how well the two agree, irrespective of the size of the areas involved. In Figure 2.2, the red box shows the ground truth area and the blue box shows the the predicted segmentation area. The area of overlap is the blue-shaded area over these two boxes as shown in the middle one in Figure 2.2, and the area of union is the blue-shaded area in the right one in Figure 2.2.

$$\text{IoU} = \frac{\text{Area of Overlap}}{\text{Area of Union}} \tag{2.7}$$

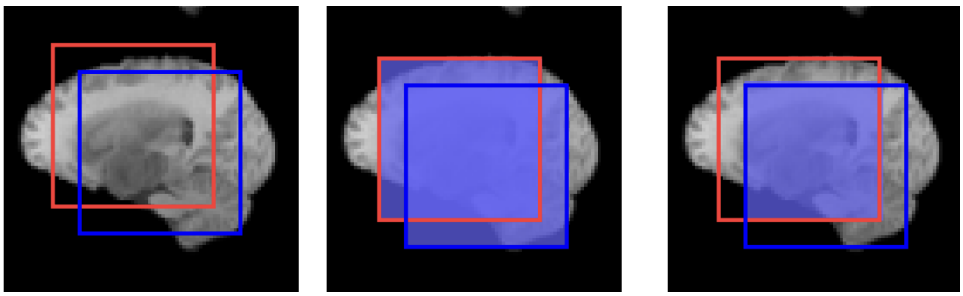

Figure 2.2 Illustration of Intersection Over Union for Brain Tumor Segmentation Task

2.4 Related Works

The recent progress in brain tumor segmentation using MR images has been significant, positioning the technology toward the forefront of medical imaging innovation. At the heart of this progress is the integration of deep learning techniques, especially the combined application of Convolutional Neural Networks (CNNs) and advanced preprocessing techniques such as Stationary Wavelet Transforms (SWT). The integration is driving a significant shift in diagnostics, resulting in tools that are not only more precise but also considerably more efficient. However, while these improvements are fascinating, their use in clinical settings is still limited. The process of transitioning from research to clinical practice is time-consuming due to rigorous validation and regulatory approvals. As a result, while the transition to these new diagnostic techniques is progressing, widespread clinical adoption remains on the horizon.

Mittal et al. [19] introduced a novel Growing Convolutional Neural Network (GCNN) model that, when combined with SWT, showed significant improvements over traditional methods such as Support Vector Machines (SVM) and conventional CNNs across various metrics, including accuracy, MSE shown as Equation 2.8, and PSNR shown as Equation 2.9. Our approach differs from this as we integrate Transfer Learning (TL) with conventional CNNs, optimizing pre-existing architectures for enhanced performance without the need for developing a new architecture from scratch. Our method utilizes established deep learning efficiencies with a focus on rapid deployment and scalability in clinical settings.

$$\text{MSE} = \frac{1}{mn} \sum_{i=1}^{m} \sum_{j=1}^{n} \left(I(i,j) - K(i,j) \right)^2 \tag{2.8}$$

where I is the original image, K is the reconstructed image, and m, n are the dimensions of the images.

$$\text{PSNR} = 10 \times \log_{10}\left(\frac{\text{MAX}_I^2}{\text{MSE}}\right) \tag{2.9}$$

where MAX_I is the maximum possible pixel value of the image. For example, in an 8-bit image, this would be 255.

Further exemplifying the advancements in this area, the application of the nnU-Net framework for brain tumor segmentation, as investigated by Fabian Isensee and colleagues [13], marks a significant milestone. Their

work not only highlights the framework's adaptability to specific segmentation tasks but also underscores its potential to enhance performance significantly, achieving commendable Dice scores and HD95 values across different tumor segmentation categories. In our study, we build directly on these findings by applying U-Net as a baseline from which we explore enhancements through preprocessing techniques and architectural tweaks for optimizing computational efficiency and model robustness in processing our specific open datasets[20][17][9][4][5].

In a similar vein, Nagwa M. Aboelenein and collaborators introduced the Hybrid Two-Track U-Net (HTTU-Net) architecture, designed to surmount the challenges of precision in automated medical diagnosis. This dual-track architecture, featuring varied layer depths and kernel sizes that merge to produce the final segmentation output, and the integration of Leaky ReLU activation and batch normalization, showcases an improved capability to efficiently process complex image datasets. The architecture contrasts with our single-path approach to Transfer Learning, where we prioritize simplicity and efficiency. However, we will analyze the potential of incorporating elements of HTTU-Net's structure to enhance segmentation detail in future iterations of our models.

Dinthisrang Daimary and his team's exploration [10] into enhancing brain tumor segmentation through hybrid Convolutional Neural Networks (CNNs) addresses the limitations of manual segmentation. They propose two innovative architectures, U-SegNet and Seg-Unet, which combine elements from the renowned U-Net and Segment models, and a third, Res-SegNet, which integrates SegNet with ResNet18 features for increased accuracy. These models utilize depth variation and skip connections inspired by U-Net to bolster feature integration, with Res-SegNet employing ResNet18's element-wise additional layer for a skip connection, showcasing the potential for accuracy improvement. This approach is similar to ours because it seeks to use the strengths of multiple architectures for improved segmentation accuracy. However, our work uses a broader dataset and specifically integrates transfer learning, allowing us to expedite training and increase data efficiency, which is crucial for our target application in real-time medical diagnostics.

The quest for efficient and accurate automatic segmentation of brain tumors from MRI images has propelled the exploration into Deep Neural Networks (DNN) due to their superior performance in image segmentation tasks. DNNs, with their multi-layered architecture, are adept at extracting features from complex datasets. Each layer in a DNN transforms one vol-

ume of activations to another from simple patterns in the initial layers to more abstract features in deep layers. It allows DNNs to capture complex details for differentiating between healthy tissue and tumor regions in brain scans.

Furthermore, DNNs often integrate convolutional layers, which are particularly effective for imaging data due to their ability to preserve spatial hierarchies and reduce the number of trainable parameters through localized receptive fields and shared weights. This architectural characteristic makes DNNs not only powerful but also efficient for processing the large datasets typically involved in medical imaging.

However, the field faced significant challenges, including issues such as gradient diffusion and the high computational demands of training deeper neural networks. Gradient diffusion, formerly known as the vanishing gradient problem, occurs during the training of deep neural networks when the gradient employed in backpropagation to update network weight decreases in magnitude as it propagates back through layers. This loss in gradient strength can result in slower convergence rates and poor network training, particularly in the deeper layers, making it more difficult to effectively capture and learn more complex patterns. Furthermore, the immense computational demands associated with training these deeper networks demand not only extensive processor capacity but also increased memory and energy usage. These problems emphasize the need for innovative approaches that enhance training efficiency and more efficiently manage computing power, allowing for the design of more powerful neural architectures.

In response, Lamia H. Shehab et al. [24] introduced an innovative approach using a Deep Residual Learning Network (ResNet) to mitigate the gradient vanishing problem typical of traditional DNNs, demonstrating notable improvements in segmentation accuracy for complete, core, and enhancing tumor regions. Our models, also incorporate residual learning principles, which are fundamental to our adopted EfficientNetB3 structure, enhancing learning depth without the risk of vanishing gradients. Similarly, Hao Chen and his team [8] proposed a novel approach for brain tumor segmentation utilizing the Deep Convolutional Symmetric Neural Network (DCSNN), incorporating symmetric masks into the deep convolutional neural network framework to address the voluminous data of MRIs and the variability in tumor appearance, highlighting the ongoing efforts to address common asymmetries in tumor regions. Our work complements their work by focusing on a balanced approach using Transfer Learning to adapt pre-trained models, which could integrate symmetric processing

techniques in subsequent refinements for enhanced accuracy.

This evolution in brain tumor segmentation technologies reflects a broader trend towards adopting more sophisticated computational models, aiming to address the multifaceted challenges in medical imaging. The cumulative efforts in this domain not only promise enhanced diagnostic capabilities but also pave the way for future innovations in medical technology.

2.5 Research Gap

The evolution of computational methods for the detection and segmentation of brain tumors from MRI scans has made significant progress, as highlighted in the existing literature. Advanced techniques in machine learning and deep learning have elevated the precision of tumor isolation and identification, improving diagnostic capabilities. However, several unaddressed challenges still limit the efficacy and applicability of current models.

First, current methods mainly focus on identifying tumor presence, location, and size. However, they fall short in differentiating complex tumor characteristics, such as distinguishing tumor cores from surrounding tissue. This limitation affects the depth of analysis required for precise medical interventions. My research aims to bridge this gap by developing a model capable of recognizing the complex tumor features and providing a more clear understanding of tumor anatomy within MRI scans.

Also, the effectiveness of computational models is inherently tied to the diversity and volume of data they are trained on. Prior studies have been constrained by limited datasets lacking variation, which impedes the model's ability to generalize across different tumor types and imaging conditions. To address the limitation, my study introduces a dataset with substantial variation, enabling the development of more robust and versatile models.

Previous approaches in tumor segmentation and classification have predominantly operated in isolation, focusing either on segmentation or classification but not both in conjunction. This separation limits the comprehensive analysis potential of these models. My research proposes an approach by integrating segmentation and classification processes, thereby enhancing the efficiency and accuracy of tumor analysis in MRI scans.

Overall, my study addresses critical gaps in knowledge, data, and methodology within the field of MRI brain tumor detection and segmentation. While recent advancements in the field have seen models achieving

an accuracy of around 98%, these often struggle with consistently differentiating tumor cores from surrounding tissues across diverse datasets. By introducing a model that excels in differentiating tumor cores from surrounding tissues with varying datasets, and integrating segmentation with classification, the research represents a significant innovation. It aims to overcome the limitations of existing models, offering a more detailed and accurate tool for medical diagnostics and treatment planning.

Chapter 3

Materials and Methods

3.1 Data Overview

3.1.1 Data Collection

This research employs several comprehensive datasets to develop and validate a Convolutional Neural Network (CNN) model enhanced by Transfer Learning (TL) techniques for the segmentation and classification of brain tumors. The datasets are sourced from publicly available repositories on Kaggle and are crucial for training our models to accurately identify and categorize brain tumors into glioma, meningioma, no tumor, and pituitary classes.

In the study, two main datasets are utilized in brain tumor MRI studies:

- **Brain Tumor MRI Dataset [20]**: The primary dataset includes 7023 images of 2D human brain MRI scans, classified into four categories: glioma, meningioma, no tumor, and pituitary. The original images vary in size and have been processed to remove extra margins to improve the model's accuracy by standardizing the input size. The dataset is sourced from a Kaggle repository created by Masoud Nickparvar and is important for the classification phase of the study.

- **BraTS 2019, 2020, 2021 Datasets [17][4][5][9]**: The BraTS datasets offer multimodal scans available in Neuroimaging Informatics Technolgy Initiative format files. The NIFTI image format is an essential standard in medical imaging, particularly for MRI data. It enables efficient storage and exchange of neuroimaging data by combining image and header information into a single file. The header includes

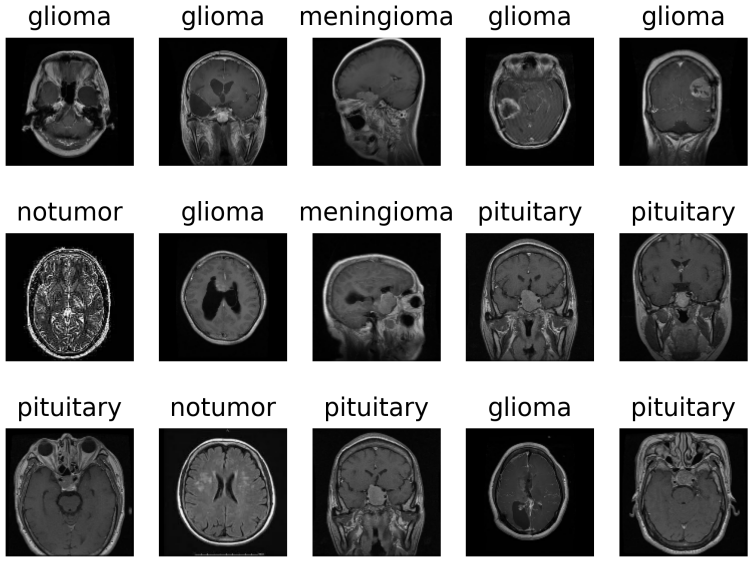

Figure 3.1 MRI Preview for Classification Model Dataset

detailed metadata crucial for data handling, such as image dimensions, orientation, and scaling. NIFTI supports both 3D spatial and 4D time-variant data arrays to facilitate precise alignment and analysis across various platforms. The scans in these datasets include native (T1), post-contrast T1-weighted (T1Gd), T2-weighted (T2), and T2 Fluid Attenuated Inversion Recovery (T2-FLAIR) volumes. These images come from various institutions and have been manually segmented by expert raters, following a consistent annotation protocol. The segmentation labels include the GD-enhancing tumor (ET), the peritumoral edema (ED), and the necrotic and non-enhancing tumor core (NCR/NET), providing a comprehensive dataset for training segmentation tasks and testing the classification model.

In the dataset[20] for classification model training, the 2D image consists of single or multi-channel pixels. However, the 3D images from BraTS dataset[17][4][5][9] are comprised of 3D cubes or voxels. In the dataset, all the 3D MRI images are stored and encoded in a NIFTI file, where each detail

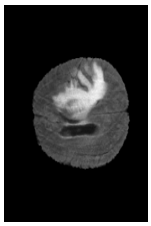

Figure 3.2 MRI Raw Image Slice from BraTS Datasets[17][4][5][9]

Figure 3.3 Mask Slice for MRI Image (left) from BraTS Datasets[17][4][5][9]

is known as an attribute. When visualizing a 3D image, a list is initialized in which, whenever a volume is read, it iterates over all 155 slices of the 3D volume to append each slice sequentially in the list. The number of voxels in a 3D image is calculated with the following equation.

$$V_t = S_t \times H_s \times W_s \tag{3.1}$$

where V_t is the total voxel number of the image, S_t is the number of 2D slices of a 3D image, H_s is the height of each slice and W_s is the width of each slice.

3.1.2 Data Preprocessing

All datasets underwent a standard preprocessing pipeline to ensure the uniformity and training efficiency of our CNN models. The process included resizing the images to a standard dimension, normalizing the pixel values, and augmenting the data to enhance model robustness against overfitting. Also, the creators of the BraTS dataset provided pre-processed data, including skull-stripped and co-registered images, to ensure consistency across training and testing sets. Given the varying dimensions of MRI images in the datasets, it is essential to standardize the size of all images to ensure uniformity in input shape for the CNN model. This process involves resizing the images to a predetermined standard size, which is 128 * 128 pixels in this study. The image processing library, OpenCV, is employed to resize the images. The interpolation method is used for the resize method considering its ability to preserve the quality of the images during resizing. In addition, the aspect ratio is maintained by padding the image with black pixels, which ensures that the images are resized to the desired dimensions without distortion. Pixel Value Normalization is also introduced in our study to scale

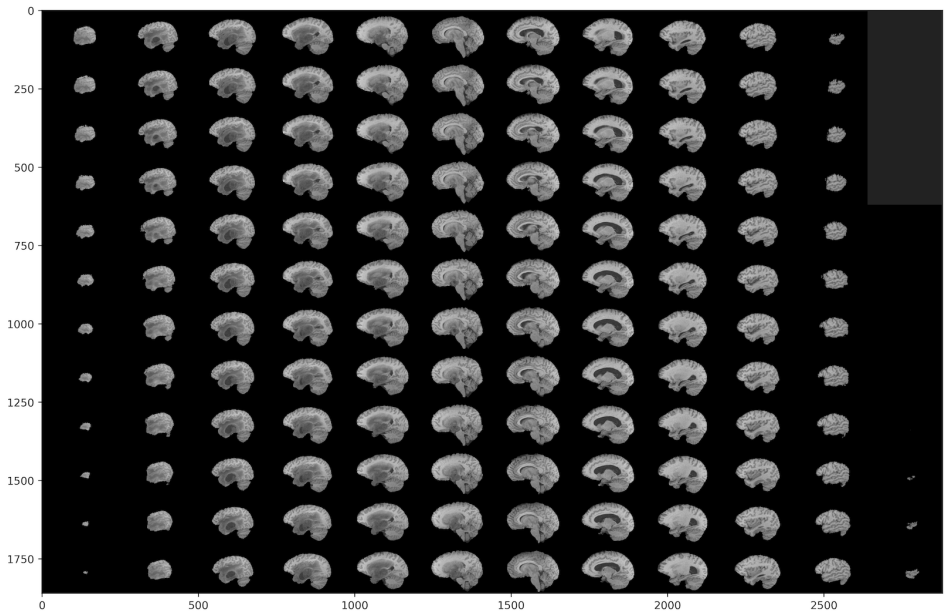

Figure 3.4 Slice graph for MRI Image [17][4][5][9]

the pixel intensity values to a common range. The pixels are normalized to the range [0, 1] by dividing each pixel value by the maximum possible intensity value, which is 255 for our images. Rotation, flipping, scaling, and translations are employed in our study to provide augmentations for the medical images. Finally, these preprocessing steps are integrated into the comprehensive data preprocessing pipeline. Thus the pipeline will automate the process of resizing, normalizing, and augmenting the images as they are loaded into the model for training, validation, or testing.

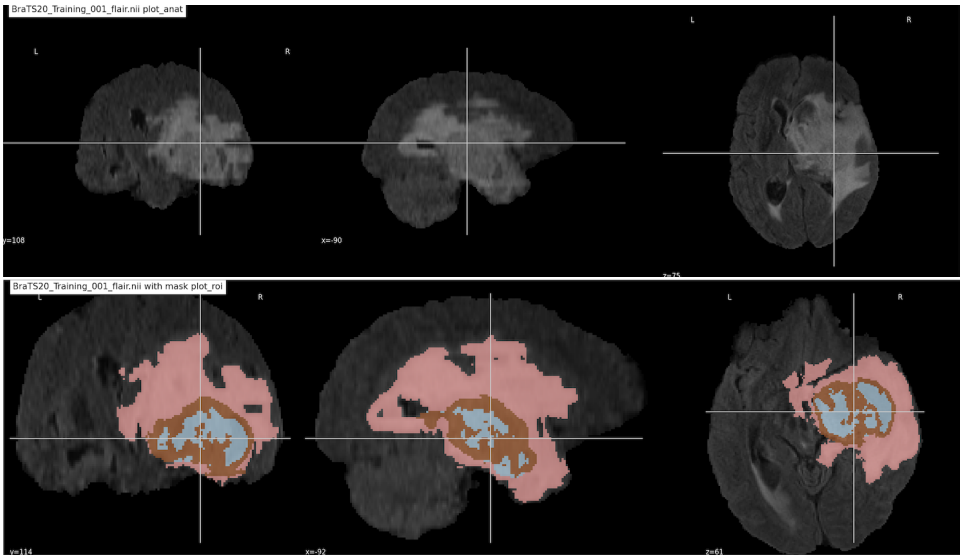

Figure 3.5 MRI Image Before Preprocessing (top row) And After ROI Enhancement (second row)[17][4][5][9]

3.2 Methodology

3.2.1 Methods Overview

Figure 3.6 illustrates the comprehensive pipeline used for the segmentation and classification of brain tumors from 3D MRI images. The first step in this pipeline involves processing the MRI images through a sophisticated 3D U-Net convolutional neural network (CNN) model. This model has been designed to detect and specify the boundaries of brain tumors by extracting essential characteristics from volumetric data. The segmented tumor areas are clearly shown in the upper right image of the figure, which highlights the precision of the tumor delineation technique.

After segmentation, the extracted tumor features are analyzed by an advanced classification model. This model employs segmented data to classify each tumor to one of multiple categories based on specified parameters. The potential categories include glioma, meningioma, pituitary, or the absence of any tumor-like signs. This classification is critical for selecting the best therapy pathway and has a substantial impact on patient prognosis.

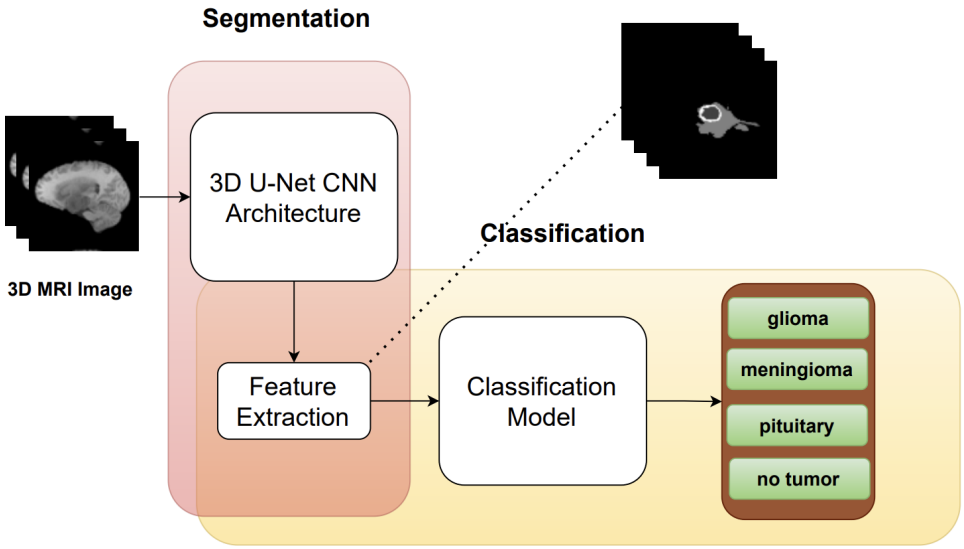

Figure 3.6 Methodology Pipeline

3.2.2 Brain Tumor Segmentation Model

The development of a CNN model based on the U-Net architecture marks a significant advancement in the segmentation of brain tumors from MRI scans. This model is designed to precisely detect tumor boundaries to improve diagnostic accuracy. It features a symmetrical structure with expanding and contracting paths to capture detailed context and localization information. This shape is crucial for identifying various tumor regions with high accuracy.

To prepare MRI images for segmentation, we perform preprocessing operations such as scaling, normalization, and data augmentation. These procedures improve the model's ability to generalize across diverse datasets and improve its performance.

Model Input Description

The input to the network consists of a grayscale image with dimensions of 128 * 128 pixels. Each pixel represents an intensity value normalized between 0 and 1, transitioning from black to white. Accompanying the input image is a mask image delineating various regions of interest within the brain. These regions include:

- GD-enhancing tumor(ET) is represented as a gray area and labeled as 1.
- Peritumoral edema(ED) is indicated by a pink color and labeled as 2.
- Non-enhancing tumor core(NET) is depicted in blue and labeled as 3.
- Areas not covered by any specific label are marked as 0, corresponding to a white background in the mask.

Model Output Description

The output from the segmentation model is a feature map that assigns a probability to each pixel. The probability indicates its likelihood of belonging to one of the following categories: GD-enhancing tumor (ET), peritumoral edema (ED), non-enhancing tumor core (NCR/NET), or a non-interest area. This probabilistic output map assists the segmentation process by highlighting the most likely category for each pixel based on the highest probability score. Consequently, each pixel is classified into the category with the maximal probability, thus defining the segmentation of the image according to the distinct pathological features.

3.2.3 U-Net Architecture Introduction

The U-Net architecture, an extension of conventional CNNs, is particularly suited for medical image segmentation due to its unique U-shaped structure. It consists of a downsampling path shown as a red arrow in Figure 3.7 to capture context and an upsampling path shown as a green arrow in Figure 3.7 for localization. The downsampling path uses convolutional and max pooling layers, the blue arrows in Figure 3.7 to reduce spatial dimensions and increase feature channels, abstracting the image into feature representations. Conversely, the upsampling path increases the output resolution, utilizing transposed convolutions, the blue arrows in Figure 3.7 and skip connections, the grey arrows in Figure 3.7 from the downsampling path to preserve spatial details critical for accurate segmentation.

The model's convolutional layers, which start with a moderate number of filters and increase progressively, use 3 * 3 kernels and ReLU activation functions to extract complex patterns indicative of tumors. This architecture is designed to maintain image dimensionality through the same padding, reduce computational demands with max pooling, and mitigate

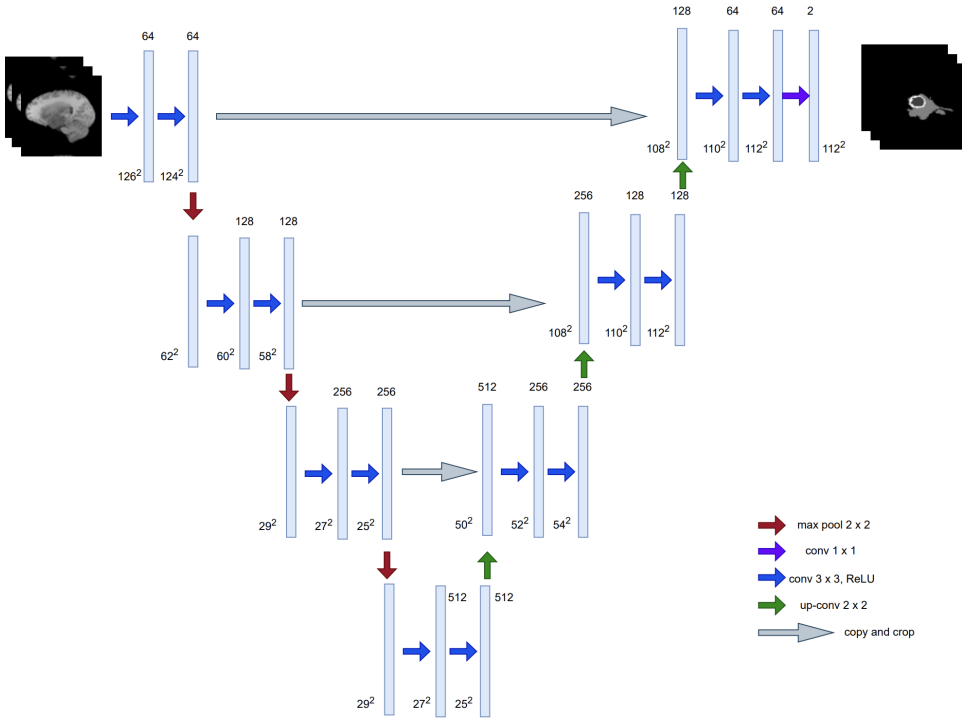

Figure 3.7 3D U-Net Architecture

over-fitting using dropout layers at strategic points. The U-Net's upsampling and concatenation techniques ensure detailed feature preservation. Upsampling reserves the resolution reduction from earlier pooling layers, reconstructing the finer details necessary for precise segmentation. Concurrently, concatenation merges these detailed feature maps with higher-level abstract features from the contracting path, reintroducing vital spatial information. This combination enriches the feature set at each stage to improve localization and reduce information loss.

The U-Net model's final 1 * 1 convolutional layer includes a softmax activation function. This function is essential in creating pixel-level probability maps for each class, converting the neural network's raw output into a form that can be easily evaluated as probabilities. Each pixel in the generated map denotes the probability that it belongs to a given category, such as a different tumor tissue. The softmax function ensures that the total of probabilities for each pixel across all classes is equal to one, allowing for more clear and confident segmentation. This function is critical for medical

diagnostics since it allows for the accurate distinction of specific tumor areas from neighboring healthy tissue.

The methodology incorporates a complicated compilation strategy designed expressly to solve the issues of medical imaging. One such difficulty is class imbalance, which happens when the quantity of samples in distinct classes differs dramatically. Class imbalance is common when segmenting brain cancers from MRI images since the areas of interest (tumors) are substantially smaller and less frequent than normal brain tissue. This imbalance can result in a model that is biased toward the majority class, decreasing sensitivity to detect malignancies. To address the issue, the model employs loss functions such as the Dice coefficient, which is intended to improve the correct identification of the minority class.

3.2.4 Brain Tumor Classification Model

Transfer learning has emerged as a pivotal technique in machine learning where annotated data are scarce and costly. This approach reuses a model developed for one task as a starting point for another based on the extensive knowledge acquired from training on large datasets. In the context of brain tumor classification, transfer learning can significantly improve both accuracy and efficiency. By adopting a model pre-trained on a vast and diverse dataset, it reduces the need for large amounts of training data, accelerating the training process while maintaining or enhancing performance.

For this study, EfficientNet B3 was selected due to its proven success in image classification tasks and architectural fit for our dataset sourced from Brain Tumor MRI Dataset[20] from Kaggle. EfficientNet B3 is also known for striking an optimal balance between computational efficiency and accuracy. Part of the EfficientNet family, EfficientNet B3 aligns perfectly with the requirements of high accuracy and manageable computational demands. This model supports the primary objective of improving diagnostic precision in classifying brain tumors, allowing for more effective treatment planning and potential clinical outcomes

The preprocessing phase prepares the dataset to meet EfficientNet B3's input specifications, resizing images to 224 * 224 pixels, normalizing pixel values, and applying data augmentation techniques to protect the model from over-fitting. The dataset is divided into training, validation, and testing sets using the train_test_split function, with 30% allocated for training and 70% reserved for testing. This distribution facilitates a comprehensive evaluation of the model's generalizability across different subsets of data.

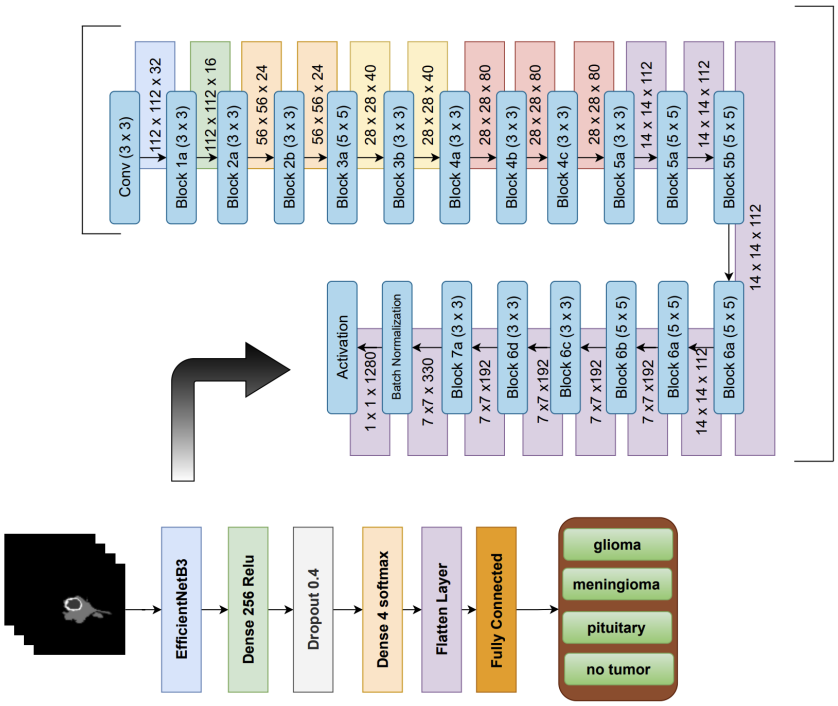

Figure 3.8 EfficientNet B3 Architecture

In adapting EfficientNet B3 for brain tumor classification, the original top layer is replaced with a fully connected layer tailored to the number of tumor classes. This customization allows the pre-trained model to meet the specific classification requirements.

Model Training and Evaluation

Both models go through meticulous training processes, with datasets separated into training, validation, and testing portions. This separation enables precise hyper-parameter adjustment and evaluation of each model's capacity to generalize to previously unseen data. The segmentation model is typically trained for 40 epochs, with changes based on performance data collected during the validation phase. During classification model training, our team actively changed the learning rate based on validation performance. To improve the model's generalizability, we used dropout layers and regularization approaches. This iterative method entailed carefully

examining the training results, followed by manual parameter adjustment before further training sessions to improve the model's performance.

The segmentation model is compiled using a combination of loss functions tailored for medical imaging, such as the Dice coefficient, which addresses issues like class imbalance. In contrast, the classification model is compiled with the Adamax Optimizer and a categorical cross-entropy loss function for its focus on multi-class classification tasks. Both models utilize optimization strategies that are best suited to their respective tasks. The Adam optimizer is chosen for segmentation for its adaptive learning rate capabilities. And the Adamax optimizer is chosen for classification because of its efficacy in handling sparse gradients.

A comprehensive set of performance metrics is employed to evaluate both models thoroughly. For the segmentation model, accuracy, precision, recall, F1-score, and the Dice coefficient are crucial for assessing effectiveness in accurately segmenting brain tumors. A higher Dice score, in particular, indicates superior segmentation performance. These metrics provide insights into each model's strengths and potential areas for improvement, highlighting the importance of precision in medical diagnostics.

Chapter 4

Result and Analysis

4.1 Results and Analysis

4.1.1 Brain Tumor Segmentation Results

Segmentation plays an important role in medical imaging for postoperative planning and early detection with the ability to divide an image into parts based on the attributes of the pixels in the image. In my work, the 3D U-net architecture is proposed for brain tumor segmentation. Figure 4.1 displays the segmentation and tumor detection for the Core part of the brain MRI image. Figure 4.2 displays the segmentation and tumor detection performance for the Enhancing part of the brain MRI Image. Both figures show the model's ability to predict the enhancing areas of brain tumors. The left side of the figure provides the ground truth, while the right side displays the model's predictions, again using a color-coded scheme for different tumor segments.

The segmentation model's core and enhancing results are depicted in Figure 4.1, where the left image represents the ground truth in black and white, and the right image illustrates the model's prediction of the core tumor area. The prediction is color-coded, with different shades—blue, green, and red—indicating various segments of the tumor's core.

Figure 4.3 illustrates the segmentation model's training journey, plotting training loss, accuracy, validation loss, and accuracy alongside metrics such as the Dice coefficient and Intersection over Union (IoU) for both training and validation datasets. The distinction between training (in blue) and validation (in red) performances shows the model's learning curve and its strong generalization capability.

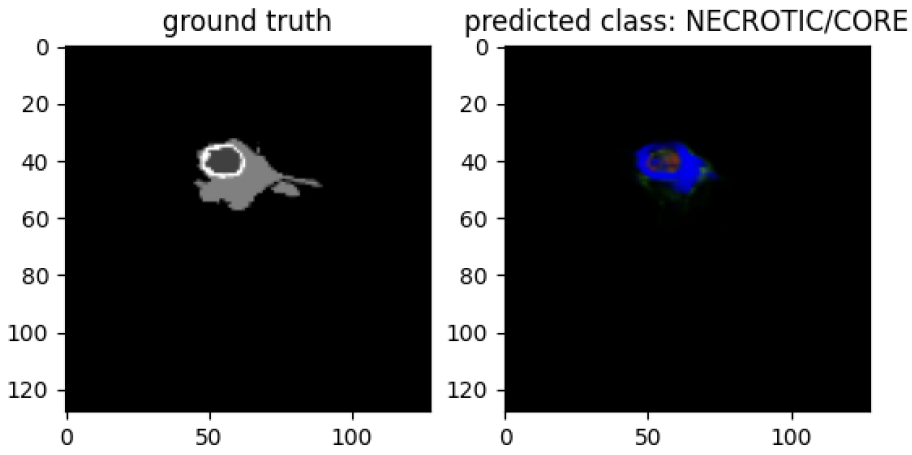

Figure 4.1 Segmentation Model CORE Result

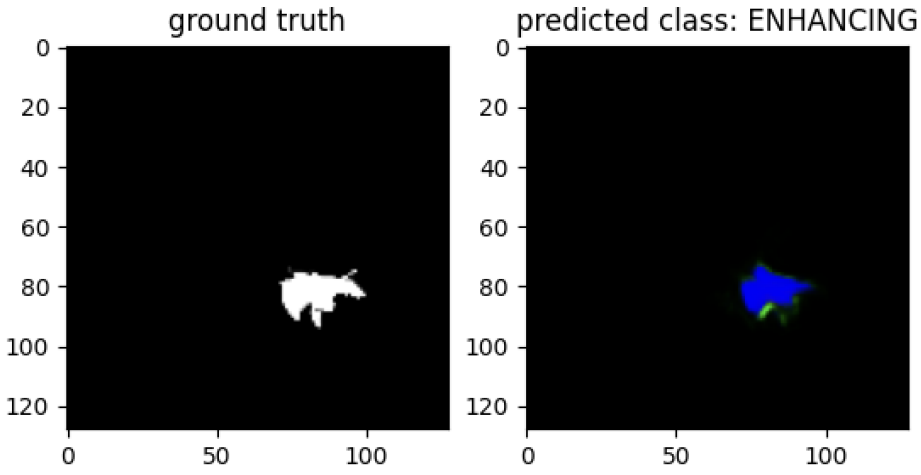

Figure 4.2 Segmentation Model Enhancing Result

As indicated in Table 4.1 and Figure 4.3, our 3D U-net segmentation model reveals excellent performance over multiple metrics, with an accuracy of 99.65%, loss rate of 0.99%, precision of 99.61%, sensitivity of 99.54%, and specificity of 99.87%, indicating that the model is effective at correctly predicting and classifying both positive and negative outcomes. However, the Dice coefficient standing at 74.86% suggests room for improvement in

Proposed Method	
Evaluation Metrics	**Performance**
Accuracy	99.65%
Dice Coefficient	74.86%
Loss	0.99%
Precision	99.61%
Sensitivity	99.54%
Specificity	99.87%

Table 4.1 Quantitative assessment of the proposed 3D U-Net Segmentation Model

the overlap between the model's predictions and the ground truth segmentation.

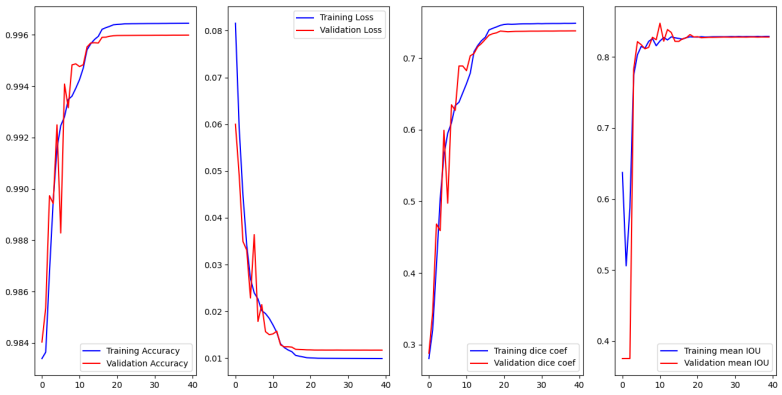

Figure 4.3 Segmentation Model Training Plot

4.1.2 Classification Results

The quantitative assessment of the proposed EfficientNet B3 Classification Model presents strong performance metrics, suggesting a highly effective model. It achieves an accuracy of 99.34%, indicating a high overall rate of correct predictions. The precision is similarly high at 99.32%, meaning that the model's positive predictions are very reliable. Notably, the model demonstrates excellent sensitivity and specificity, at 99.78% and 99.80% re-

spectively, which indicates that it is exceptionally adept at correctly identifying true positives and true negatives, crucial for minimizing false detection in practical applications. The low loss rate of 0.86% further underscores the model's ability to closely approximate the true labels, confirming its robust predictive capability. These results highlight the model's effectiveness in classification tasks, making it a strong candidate for applications requiring high precision and reliability.

Proposed Method	
Evaluation Metrics	**Performance**
Accuracy	99.34%
Loss	0.86%
Precision	99.32%
Sensitivity	99.78%
Specificity	99.80%

Table 4.2 Quantitative assessment of the proposed EfficientB3 Classification Model

In Figure 4.4, the graph illustrates the training and validation trajectory of the classification model, showing how both accuracy and loss converge over the epochs. The green line represents validation accuracy, while the red line indicates training accuracy, demonstrating their progression as training continues. Notably, the training loss reaches its optimal value at epoch 19, and the training accuracy peaks at 99% by epoch 14. Importantly, there is no evidence of over-fitting in this scenario. Over-fitting occurs when a model learns the details and noise in the training data to the extent that it negatively impacts the performance of the model on new data, typically shown by a divergence between training and validation metrics. However, in this case, the close alignment of the training and validation lines throughout the process indicates that the model generalizes well to unseen data, maintaining robust performance without over-fitting.

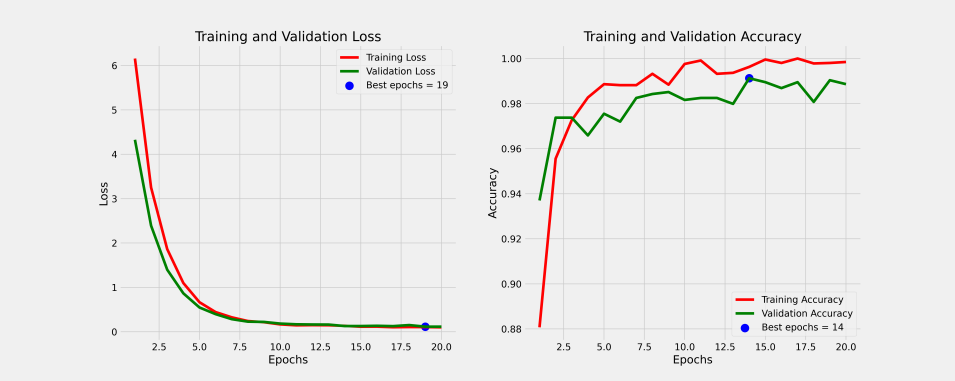

Figure 4.4 Classification Model Training Plot

4.1.3 Limitations and Future Works

The major limitations of the study are as follows:

- Model Complexity and Computational Demand: The sophisticated models require substantial computational resources, which limits deployments in less-equipped medical facilities.
- Handling of Rare Tumor Types: The model may not perform well when encountering rare or atypical brain tumors not well-represented in the training datasets. The limitation might affect the utility in diverse clinical scenarios, where rare tumors might present.
- Variability in Image Acquisition Parameters: MRI scans can vary based on the machine's manufacturer, model, or settings used during the imaging process. These variations can affect image quality and contrast, potentially leading to inconsistent model performance in different healthcare settings.

In the future, we will manage to incorporate a wider variety of imaging data from different demographics and machines to improve the model's generalizability. Also, we aim to develop real-time, automated diagnostic systems that integrate with hospital MRI hardware which can significantly speed up the diagnosis process.

Chapter 5

Conclusion

5.1 Conclusion

The integration of image-processing ability with diagnostic computer systems has revolutionized the field of medical radiology, significantly accelerating the diagnosis process while enhancing patient outcomes concurrently. Numerous methods for brain tumor segmentation and classification have been developed to improve the accuracy and efficiency of medical image analysis. Despite their potential, these techniques often encounter challenges such as poor image contrast, inaccuracies in tumor region segmentation due to artifacts, the computational intensity of the methods which prolongs the diagnosis time, and the requirement for extensive training data in existing deep learning models.

The proposed brain tumor segmentation and classification algorithms aim to address the concerns mentioned above. In our study, we use 3D U-Net architecture for precise tumor boundary delineation and an EfficientNet B3 model for robust tumor type classification, with a focus on glioma, meningioma, no tumor, and pituitary tumor categories.

In both the segmentation model and the classification model, we achieve an impressive accuracy of over 99%, underscoring the effectiveness of integrating CNN architectures and transfer learning techniques to address the challenges in brain tumor diagnosis over tumor appearance. The use of large-scale, diverse datasets, including MRI images from open-accessible archives, enabled the training of models not only to perform well under controlled conditions but also to demonstrate robustness across different clinical imaging scenarios.

Looking ahead, we plan to address the limitations identified in our study, including the model complexity and computational demands, as well as the handling of rare tumor types and the variability in image acquisition parameters. Our future work will focus on incorporating a wider variety of imaging data from different demographics and machines to enhance the model's generalizability. Additionally, we aim to develop a real-time, automated diagnostic system that integrates directly with hospital MRI hardware, which could further accelerate the diagnostic process.

Bibliography

[1] Nagwa M. Aboelenein, Piao Songhao, Anis Koubaa, Alam Noor, and Ahmed Afifi. Httu-net: Hybrid two track u-net for automatic brain tumor segmentation. *IEEE Access*, 8:101406–101415, 2020.

[2] Nagwa Aboelenien, Piao Songhao, Anis Koubaa, Alam Noor, and Ahmed Afifi. Httu-net: Hybrid two track u-net for automatic brain tumor segmentation. *IEEE Access*, PP:1–1, 05 2020.

[3] Ehab F Badran, Esraa Galal Mahmoud, and Nadder Hamdy. An algorithm for detecting brain tumors in mri images. In *The 2010 International Conference on Computer Engineering & Systems*, pages 368–373. IEEE, 2010.

[4] Spyridon Bakas, Hamed Akbari, Aristeidis Sotiras, Michel Bilello, Martin Rozycki, Justin S. Kirby, John B. Freymann, Keyvan Farahani, and Christos Davatzikos. Advancing the cancer genome atlas glioma mri collections with expert segmentation labels and radiomic features. *Scientific Data*, 4(1), Sep 2017.

[5] Spyridon Bakas, Mauricio Reyes, Andras Jakab, Stefan Bauer, Markus Rempfler, Alessandro Crimi, Russell Takeshi Shinohara, Christoph Berger, Sung Min Ha, Martin Rozycki, Marcel Prastawa, Esther Alberts, Jana Lipkova, John Freymann, Justin Kirby, Michel Bilello, Hassan Fathallah-Shaykh, Roland Wiest, Jan Kirschke, and Benedikt Wiestler. Identifying the best machine learning algorithms for brain tumor segmentation, progression assessment, and overall survival prediction in the brats challenge. *arXiv:1811.02629 [cs, stat]*, Apr 2019.

[6] Debnath Bhattacharyya and Tai-hoon Kim. Brain tumor detection using mri image analysis. In *Ubiquitous Computing and Multimedia Ap-*

plications: Second International Conference, UCMA 2011, Daejeon, Korea, April 13-15, 2011. Proceedings, Part II 2, pages 307–314. Springer, 2011.

[7] Satish Chandra, Rajesh Bhat, and Harinder Singh. A pso based method for detection of brain tumors from mri. In *2009 World Congress on Nature & Biologically Inspired Computing (NaBIC)*, pages 666–671. IEEE, 2009.

[8] Hao Chen, Zhiguang Qin, Yi Ding, Lan Tian, and Zhen Qin. Brain tumor segmentation with deep convolutional symmetric neural network. *Neurocomputing*, 392:305–313, 2020.

[9] Kenneth Clark, Bruce Vendt, Kirk Smith, John Freymann, Justin Kirby, Paul Koppel, Stephen Moore, Stanley Phillips, David Maffitt, Michael Pringle, Lawrence Tarbox, and Fred Prior. The cancer imaging archive (tcia): Maintaining and operating a public information repository. *Journal of Digital Imaging*, 26(6):1045–1057, Jul 2013.

[10] Dinthisrang Daimary, Mayur Bhargab Bora, Khwairakpam Amitab, and Debdatta Kandar. Brain tumor segmentation from mri images using hybrid convolutional neural networks. *Procedia Computer Science*, 167:2419–2428, 2020. International Conference on Computational Intelligence and Data Science.

[11] Selvaraj Damodharan and Dhanasekaran Raghavan. Combining tissue segmentation and neural network for brain tumor detection. *Int. Arab J. Inf. Technol.*, 12(1):42–52, 2015.

[12] Vijay P.B. Grover, Joshua M. Tognarelli, Mary M.E. Crossey, I. Jane Cox, Simon D. Taylor-Robinson, and Mark J.W. McPhail. Magnetic resonance imaging: Principles and techniques: Lessons for clinicians. *Journal of Clinical and Experimental Hepatology*, 5(3):246–255, Sep 2015.

[13] Fabian Isensee, Paul F. Jäger, Peter M. Full, Philipp Vollmuth, and Klaus H. Maier-Hein. nnu-net for brain tumor segmentation. *Brainlesion: Glioma, Multiple Sclerosis, Stroke and Traumatic Brain Injuries*, page 118–132, 2021.

[14] Ahmed Kharrat, Nacéra Benamrane, Mohamed Ben Messaoud, and Mohamed Abid. Detection of brain tumor in medical images. In *2009 3rd International conference on signals, circuits and systems (SCS)*, pages 1–6. IEEE, 2009.

[15] Hassan Khotanlou, Olivier Colliot, Jamal Atif, and Isabelle Bloch. 3d brain tumor segmentation in mri using fuzzy classification, symmetry analysis and spatially constrained deformable models. *Fuzzy sets and systems*, 160(10):1457–1473, 2009.

[16] Subhranil Koley and Aurpan Majumder. Brain mri segmentation for tumor detection using cohesion based self merging algorithm. In *2011 IEEE 3rd International Conference on Communication Software and Networks*, pages 781–785. IEEE, 2011.

[17] Bjoern H. Menze, Andras Jakab, Stefan Bauer, Jayashree Kalpathy-Cramer, Keyvan Farahani, Justin Kirby, Yuliya Burren, Nicole Porz, Johannes Slotboom, Roland Wiest, Levente Lanczi, Elizabeth Gerstner, Marc-Andre Weber, Tal Arbel, Brian B. Avants, Nicholas Ayache, Patricia Buendia, D. Louis Collins, Nicolas Cordier, and Jason J. Corso. The multimodal brain tumor image segmentation benchmark (brats). *IEEE Transactions on Medical Imaging*, 34(10):1993–2024, Oct 2015.

[18] Richa Mishra. Mri based brain tumor detection using wavelet packet feature and artificial neural networks. In *Proceedings of the International Conference and Workshop on Emerging Trends in Technology*, pages 656–659, 2010.

[19] Mamta Mittal, Lalit Mohan Goyal, Sumit Kaur, Iqbaldeep Kaur, Amit Verma, and D Jude Hemanth. Deep learning based enhanced tumor segmentation approach for mr brain images. *Applied Soft Computing*, 78:346–354, 2019.

[20] Msoud Nickparvar. Brain tumor mri dataset, 2021.

[21] National Institute of Biomedical imaging and bioengineering. Magnetic resonance imaging (mri), Jul 2018.

[22] Roger J Packer, Henry S Friedman, Larry E Kun, and Gregory N Fuller. Tumors of the brain stem, cerebellum, and fourth ventricle. *Cancer in the nervous system*, pages 171–192, 2002.

[23] Sudipta Roy, Sanjay Nag, Indra Kanta Maitra, and Samir Kumar Bandyopadhyay. A review on automated brain tumor detection and segmentation from mri of brain. *arXiv preprint arXiv:1312.6150*, 2013.

[24] Lamia H. Shehab, Omar M. Fahmy, Safa M. Gasser, and Mohamed S. El-Mahallawy. An efficient brain tumor image segmentation based on deep residual networks (resnets). *Journal of King Saud University - Engineering Sciences*, 33(6):404–412, Sep 2021.

[25] A Aria Tzika, Loukas Astrakas, and Maria Zarifi. Pediatric brain tumors: Magnetic resonance spectroscopic imaging. *Diagnostic Techniques and Surgical Management of Brain Tumors*, 205, 2011.